

Real-to-Sim: Deep Learning with Auto-Tuning to Predict Residual Errors using Sparse Data

Alexander Schperberg¹, Yusuke Tanaka¹, Feng Xu¹,
Marcel Menner², and Dennis Hong¹

Abstract—Achieving highly accurate kinematic or simulator models that are close to the real robot can facilitate model-based controls (e.g., model predictive control or linear-quadratic regulators), model-based trajectory planning (e.g., trajectory optimization), and decrease the amount of learning time necessary for reinforcement learning methods. Thus, the objective of this work is to learn the residual errors between a kinematic and/or simulator model and the real robot. This is achieved using auto-tuning and neural networks, where the parameters of a neural network are updated using an auto-tuning method that applies equations from an Unscented Kalman Filter (UKF) formulation. Using this method, we model these residual errors with only small amounts of data — a necessity as we improve the simulator/kinematic model by learning directly from hardware operation. We demonstrate our method on robotic hardware (e.g., manipulator arm), and show that with the learned residual errors, we can further close the reality gap between kinematic models, simulations, and the real robot.

I. INTRODUCTION

One of the primary challenges in the field of robotics is to successfully exploit simulation-based results and apply these results to real-world applications. Simulations are convenient as they provide data with low-cost, and can be run safely for long periods of time without risking potentially expensive hardware. However, in almost all cases (even for high-fidelity and expensive simulators), the simulation and reality will differ, i.e., ‘reality gap’, due to error or mismatch from sensors and actuators that are difficult to correctly model. Because of this reality gap, it typically takes a significant amount of engineering effort to successfully train an agent in simulation and then transfer this learning to hardware. In previous work (see Section II), there have been numerous approaches to close this reality gap [1], however, these approaches still require intricate hand-tuning and substantial data collection. Ideally, one way to close the reality gap is to either have an accurate kinematic/dynamic model of the robot itself and/or directly use hardware data to inform, and improve the simulator. Still, the challenge remains in that access to a highly accurate kinematic/dynamic model is difficult and typically only sparse amounts of data can be received from hardware experiments. Thus, methods that



Fig. 1. **Real-to-Sim.** Here we show our experimental setup, where a manipulator robot is used to learn the residual error between the actual and simulated robot.

can quickly improve a kinematic model, or a simulator using sparse amounts of data are needed.

In this work, our objective is to provide a method to learn the residual errors assumed to be non-linear and non-Gaussian between a simple kinematic or simulator model, and the real robot. By learning these residual errors, we can either improve an existing kinematic model to be closer to the real robot, or improve the simulator to be closer to the real robot. The former may be useful for model-based controls (e.g., model predictive control) or for model-based planners, while the latter can be used for reinforcement learning (RL) applications. The residual errors are learned using deep learning, where the parameters of a neural network are updated with a state-of-the-art auto-tuning method [2], which can quickly converge to desired parameters (i.e., minimizing the difference between the current and reference model) through an Unscented Kalman Filter (UKF). A UKF is useful (relative to other filtering methods) as they can better handle non-linear and non-Gaussian residual errors.

Summary of our contributions

- 1) An implementation of neural networks with auto-tuning is used to quickly learn residual errors between the current and reference model.
- 2) We show how our method learns the residual error for several test cases, in particular Sim-to-Kin (simulator is the reference model and the kinematics with residual error is the current model), Real-to-Kin (the real robot is the reference model and the kinematics with residual error is the current model), and Real-to-Sim (the real robot is the reference model and the simulator with residual error is the current model).
- 3) Our results are demonstrated in simulation and hardware using a mobile and stationary robot.

¹A. Schperberg, Y. Tanaka, F. Xu, and D. Hong are with the Robotics and Mechanisms Laboratory, Department of Mechanical and Aerospace Engineering, University of California, Los Angeles, CA, USA 90095 {aschperberg28, yusuketanaka, xufengmax, dennishong}@ucla.edu

²M. Menner is with Mitsubishi Electric Research Laboratories (MERL), Cambridge, MA, 02139, USA. menner@ieee.org

II. RELATED WORKS

The reality gap between policies trained in simulations and then applied to real-world tasks are typically addressed through domain randomization, domain adaptation, or system identification methods. In domain randomization, a model is trained across simulated environments that vary in its dynamics or visual information. The real-world environment is then assumed to be generalizable as a sub-variant of these randomized environments [3]. However, as sample complexity exponentially increases with the number of randomizations, the work in [4] has shown that domain randomization (in general) leads to suboptimal and high variance policies. To resolve the increase of sample complexity over time, [5] addresses this through automatic domain randomization, which expands the range of parameters autonomously during the agent’s learning procedure. However, by not using real-world data, their final distribution of parameters may not sufficiently reflect the actual distribution of the real world – a common issue among many sim-to-real works [3].

Another approach is to use real-world data directly to influence simulation parameters. For example, [6] uses continuous object tracking with real-world data to compare trajectories between the real and simulated model. Other works have also employed model-based RL and use real-world data to learn a policy that fits some probabilistic model [7], [8]. Still, using machine learning only on real-world data to address the reality gap can be time consuming and impractical depending on the task or environment complexity, as current methods rely on sufficient data collection and may lead to safety issues for real robots during the training execution.

A hybrid approach (between using real-world and simulated data) exists through domain adaptation methods. [9] achieves desired manipulation tasks by learning a policy on the real robot through collection of unlabeled real-world images, which are then employed along with simulated images to adapt the policy (effectively decreasing the number of real-world data required). However, while [9] does not improve the simulator itself during the learning process, [3] does improve the simulator by matching reality and reduces (over time) the need for real-world data. Although this hybrid approach has been used with success, it requires a careful and often times complex procedure for generating new simulation data, and the agent’s policy may struggle to learn if the distribution of the simulation parameters grow too large [9], [10]. Thus, while RL has made significant progress in the field of sim-to-real applications, resolving real-world data sparsity along with generalizing the training process across environments/robots remains a consistent issue.

Another approach is to apply methods of system identification and Bayesian optimization, such as in [11] which use prior knowledge of the system. These works typically only account for geometric parameters and do not consider non-linearities that arise from kinematic chains and noise in system propagation (although these methods benefit from being applicable on the real world directly without learning

requirements). Further, to achieve the accuracy required in the task-relevant state-space domain, non-geometric errors need to be accounted for including friction, temperature, and compliance which is difficult and potentially infeasible to model without learning-based methods [12], [13].

In this work, our goal is to make it feasible to train on real-world data directly to continuously improve the simulated model, i.e., real-to-sim (or sometimes referred to as modelling a ‘digital twin’ [13]) using a learning-based auto-tuning approach. Other works similar to our goal but different in approach can be found in [14], where the forward kinematics are modeled by optimizing Denavit–Hartenberg parameters through standard gradient descent (SGD) methods. Our work differs as we are not restricted to robots with only revolute or prismatic joints but is generalizable to any robot type (e.g., wheeled robots). Another work in this space is found in [10] which learns the non-parametric model error in addition to the existing (uncalibrated) forward model. Similar to our work, [10] applies a trade-off between modelling the non-geometric effects by hand and removing the available kinematic model completely. They achieve this through obtaining accurate forward models in the presence of non-linearities by learning residual errors using Gaussian Process Regression (GPR). However, because these residual errors (or in our case, model mismatch from proprioceptive and exteroceptive noise) is not only non-linear but non-Gaussian, we opt for neural networks instead.

Ultimately, our approach is to directly learn the model or residual error between a desired or reference model and the current model. The reference or current model may be composed of a simple kinematic model, the state feedback of the simulator, or the state feedback of the real robot (in our case either a mobile or 6 degrees of freedom manipulator robot). To learn this model error we employ the auto-tuning method described in [2], which uses a Kalman filter to predict control parameters with user-defined training objectives to evaluate the performance of a closed-loop system online through a recursive implementation. This method has previously shown success for multiple applications, from tuning the cost function weights of an LQR controller for autonomous vehicles [2] to tuning a model predictive controller and trajectory planner of a quadruped robot [15]. Here, we apply this method for tuning the weights of a neural network toward learning the model error. We use a neural network because we assume this model error is non-linear and non-Gaussian and may potentially learn semantic information that is difficult to account for manually. The motivation of using this auto-tuning method (against RL for example), is because this approach utilizes an Unscented Kalman Filter (UKF) for updating control parameters—thus, the method requires small amounts of data to quickly update parameters (which is necessary as we plan to learn directly from real-world data). Additionally, because this approach is applied online and recursively, the auto-tuner can quickly adapt to new changes (i.e., model changes or sudden change in the localization result that affects the model error).

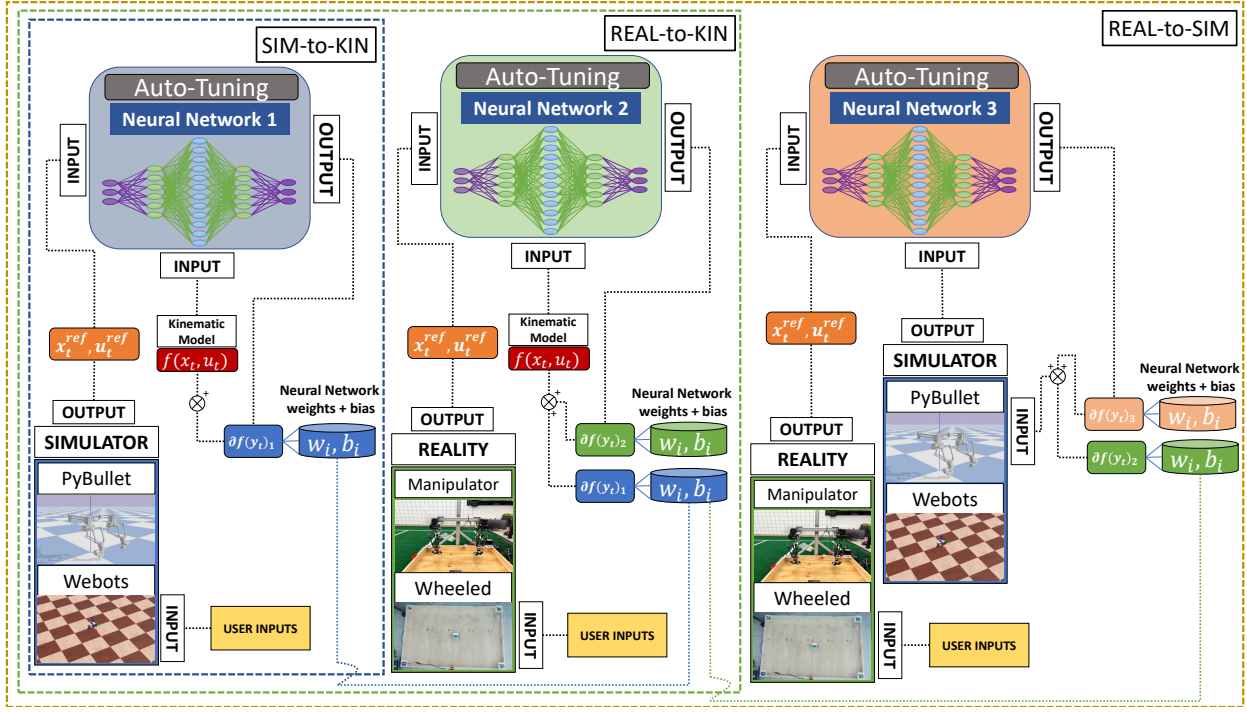


Fig. 2. **Methods flowchart.** Here we show the overall methods of this paper as described in Section III. Overall, the goal is to learn the residual model error between a simulator model and a kinematic model or Sim-to-Kin (boxed in blue), the real robot and a kinematic model or Real-to-Kin (boxed in green), and the real robot and the simulator model or Real-to-Sim (boxed in brown). The model is learned using an auto-tuning method which calibrates weights and bias parameters of a neural network. Although not necessary, the learned residual model of one case may also be used as part of the next case (e.g., the residual model for Sim-to-Kin may be used as the starting residual error for the Real-to-Kin case—potentially reducing the amount of learning required to model any additional residual error).

III. PROBLEM DEFINITIONS

A. General Model

We assume the following model propagation from time step t to $t + 1$:

$$\mathbf{x}_{t+1} = f(\mathbf{x}_t, \mathbf{u}_t) + \delta f(\mathbf{y}_t) \quad (1)$$

where \mathbf{x}_t is the state, \mathbf{u}_t is the control input, $f(\mathbf{x}_t, \mathbf{u}_t)$ is some kinematic model, and $\delta f(\mathbf{y}_t)$ is considered the model mismatch (or residual error of the model), which we assume to be a non-Gaussian and non-linear function parameterized by \mathbf{y}_t . Note, throughout this paper, we will model the derivative terms of the system dynamics since our environment is assumed uniform, and the residual term is not a function of positional space. The objective of this paper is to learn the function $\delta f(\mathbf{y}_t)$ through a neural network with auto-tuning (see Section III-B). Here, we will learn the residual error for several different cases, and transfer the learned residual from one case to the next case to help decrease the overall learning time. Note that from this point, we will use the hat notation on states that result from a predicted model (i.e., kinematic model with the addition of a residual error) and a bar on states that are received directly from the localization result of the simulation or the real robot.

Our first test case will be Sim-to-Kin, where we use a predefined kinematic model, $f(\mathbf{x}_t, \mathbf{u}_t)$, and learn the residual error $\delta f(\mathbf{y}_t)_1$ to predict the state of the model of a simulation, $\hat{\mathbf{x}}_{t+1}^{sim}$. Thus, we can write the Sim-to-Kin case as the

following:

$$\hat{\mathbf{x}}_{t+1}^{sim} = f(\mathbf{x}_t, \mathbf{u}_t) + \delta f(\mathbf{y}_t)_1 \quad (2)$$

The next test case will be Real-to-Kin, where we try to match a kinematic model to the results of the real robot. For this case, instead of starting with just the kinematic model, $f(\mathbf{x}_t, \mathbf{u}_t)$, we instead apply the learned residual from equation (2) in addition to the kinematic model, and learn the remaining (new) residual specified as $\delta f(\mathbf{y}_t)_2$. Note, by using the previously learned model as the updated Kinematic model, we may decrease the amount of training time needed to find the remaining residual error – however, this is only true if we assume that the simulator model is more accurate than the initialized kinematic model as we do in this paper (although this is not a prerequisite to using our methods and the previously learned model may also be set to zero if equation (3) is not true):

$$|\bar{\mathbf{x}}_{t+1}^{real} - f(\mathbf{x}_t, \mathbf{u}_t)| > |\bar{\mathbf{x}}_{t+1}^{real} - \hat{\mathbf{x}}_{t+1}^{sim}| \quad (3)$$

The Real-to-Kin case can then be specified as:

$$\hat{\mathbf{x}}_{t+1}^{real} = f(\mathbf{x}_t, \mathbf{u}_t) + \delta f(\mathbf{y}_t)_1 + \delta f(\mathbf{y}_t)_2 \quad (4)$$

where the goal is to learn the residual error, $\delta f(\mathbf{y}_t)_2$, while $\delta f(\mathbf{y}_t)_1$ was already learned from the previous Sim-to-Kin case.

Lastly, we will test the Real-to-Sim case, where our goal is to match the simulator model to the real robot. As

before, we can make use of the previously learned cases to inform and facilitate the training procedure. For example, we can combine equations (2) and (4) to get the following relationship (with the goal of finding the remaining new residual error $\delta f(\mathbf{y}_t)_3$):

$$\hat{\mathbf{x}}_{t+1}^{real} = f(\mathbf{x}_t, \mathbf{u}_t) + \delta f(\mathbf{y}_t)_1 + \delta f(\mathbf{y}_t)_2 + \delta f(\mathbf{y}_t)_3 \quad (5)$$

which can be simplified through:

$$\hat{\mathbf{x}}_{t+1}^{real} = \hat{\mathbf{x}}_{t+1}^{sim} + \delta f(\mathbf{y}_t)_2 + \delta f(\mathbf{y}_t)_3 \quad (6)$$

However, we note that in this test case we assume that both the simulator and the real robot are running simultaneously, thus, we assume access to the actual simulator states during the training procedure, and we don't need to rely on a predicted model of the simulator. Thus, we replace the predicted simulator model, $\hat{\mathbf{x}}_t^{sim}$, with the actual simulator values defined by $\bar{\mathbf{x}}_t^{sim}$ (in this case, $\delta f(\mathbf{y}_t)_2$ may act as a 'warm-start' for modeling the behavior of the real robot, since the term was learned during Real-to-Kin):

$$\hat{\mathbf{x}}_{t+1}^{real} = \bar{\mathbf{x}}_t^{sim} + \delta f(\mathbf{y}_t)_2 + \delta f(\mathbf{y}_t)_3 \quad (7)$$

B. Neural Network with Auto-Tuning

As described previously, the goal is to learn the residual error $\delta f(\mathbf{y}_t)$ from equation (1) in order to minimize the difference between the current and a reference model. Depending on the test case, what is designated as the current and reference model may differ. For example, in Sim-to-Kin the reference model is the simulator while the current model is the specified kinematics, in Real-to-Kin, the reference model is the real robot while the current model is the specified kinematics, and in Real-to-Sim, the reference model is the real robot while the current model is the simulator model. Each of these cases and which specific residual model we wish to learn is described in Section (III-A).

To learn this residual error $\delta f(\mathbf{y}_t)$ we use a fully connected Neural Network (see Fig. 3) that has one input layer (with either 5 inputs when using our mobile robot or 6 inputs when using our manipulator robot), one hidden layer with 10 nodes, and one output layer (with 3 outputs when using our mobile or manipulator robot). We can write this network as the following:

$$\delta(f(\mathbf{y})) = \mathbf{y}_{out} \sigma \left(\mathbf{y}_{lay} \sigma \left(\mathbf{y}_{in} \mathbf{z} + \mathbf{y}_{in,0} \right) + \mathbf{y}_{lay,0} \right) + \mathbf{y}_{out,0} \quad (8)$$

where $\mathbf{y}_{out} \in \mathbb{R}^{3 \times 10}$ are the weights of the output layer, $\mathbf{y}_{out,0} \in \mathbb{R}^{3 \times 1}$ are the bias of the output layer, $\mathbf{y}_{lay} \in \mathbb{R}^{10 \times 10}$ are the weights of the hidden layer, $\mathbf{y}_{lay,0} \in \mathbb{R}^{10 \times 1}$ are the bias of the hidden layer, $\mathbf{y}_{in} \in \mathbb{R}^{5 \times 10}$ or $\mathbb{R}^{6 \times 10}$ are the weights of the input layer, and $\mathbf{y}_{in,0} \in \mathbb{R}^{5 \times 1}$ or $\mathbb{R}^{6 \times 1}$ are the bias of the input layer, and lastly, the inputs are represented by $\mathbf{z} \in \mathbb{R}^{5 \times 1}$ or $\mathbb{R}^{6 \times 1}$. Thus, in total, $\delta(f(\mathbf{y}))$ is a function parameterized by $\mathbf{y} \in \mathbb{R}^{198 \times 1}$ for the mobile robot, and $\mathbf{y} \in \mathbb{R}^{209 \times 1}$ for the robot manipulator. The σ represent leaky ReLu activation functions $\mathbf{a} = \sigma(\mathbf{b})$ with $\mathbf{a} = \max(0.01\mathbf{b}, \mathbf{b})$.

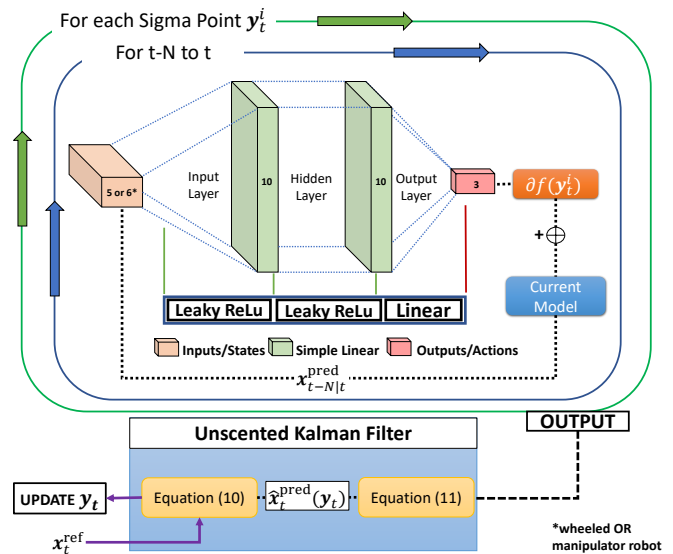


Fig. 3. **Neural Network with Auto-Tuning.** We illustrate the auto-tuning method as described in Section III-B. The auto-tuner calibrates weights and bias values of a neural network that is composed of a hidden layer. The result of this calibration is to produce an output or residual model error that minimizes the difference between a current and reference model.

Equation (8) is considered the feed-forward procedure of a neural network. However, in this paper, instead of using typical back-propagation methods with optimization functions such as Batch Gradient Descent or ADAM, we instead apply the auto-tuning method described in [2]. The motivation of using this auto-tuning method opposed to other more typical back-propagation methods is that it's model-based and has been shown in previous works [15], [16] to tune parameters quickly with sparse amounts of data. Because in most cases we have some idea of what the model of our system looks like (e.g., wheeled robots with a differential drive model, or manipulator robot that utilizes forward/inverse kinematics), we can decrease the amount of residual error that needs to be learned by incorporating this model into the training procedure (whereas model-free methods would require large amounts of data to potentially first match a predefined kinematic model before improving upon this model). Decreasing the training time is critical for our application as we seek to learn the residual error between the real robot and a simulator (or kinematic model) using data directly from the real robot (i.e., the amount of data we can collect will be limited).

While we refer the reader to [2] for a full description of this auto-tuning method, the main objective of this method will be to tune the control parameters \mathbf{y}_t (where t is the current time step) such that the difference between a predicted model, \mathbf{x}_t^{pred} , and a reference model, \mathbf{x}_t^{ref} , is minimized. This calibration is done through finding a Kalman gain \mathbf{K}_t through an Unscented Kalman Filter (UKF) using a recursive implementation. In other words, we first collect the history of past reference and localization values using a time horizon specified by $t - N$ (where N is the number of time steps

in the past time horizon), and make the Kalman gain update at the current time step t . Thus, we formulate the update of our control parameter as:

$$\mathbf{y}_t = \mathbf{y}_{t-N} + \Delta \mathbf{y}_t, \quad (9)$$

where the update $\Delta \mathbf{y}_t$ is computed based on the following equation:

$$\Delta \mathbf{y}_t = \mathbf{K}_t \left(\mathbf{x}_t^{\text{ref}} - \hat{\mathbf{x}}^{\text{pred}}(\mathbf{y}_t) \right) \quad (10)$$

Finally, the Kalman gain is calculated using the following UKF formulation:

$$\mathbf{K}_t = \mathbf{C}_t^{sz} \mathbf{S}_t^{-1} \quad (11a)$$

$$\mathbf{S}_t = \mathbf{C}_v + \sum_{i=0}^{2L} \mathbf{w}^{c,i} (\mathbf{x}_t^{\text{pred},i} - \hat{\mathbf{x}}_t^{\text{pred}}) \quad (11b)$$

$$(\mathbf{x}_t^{\text{pred},i} - \hat{\mathbf{x}}_t^{\text{pred}})^\top \quad (11c)$$

$$\mathbf{C}_t^{sz} = \sum_{i=0}^{2L} \mathbf{w}^{c,i} (\mathbf{y}_t^i - \hat{\mathbf{y}}_t) (\mathbf{x}_t^{\text{pred},i} - \hat{\mathbf{x}}_t^{\text{pred}})^\top \quad (11d)$$

$$\hat{\mathbf{x}}_t^{\text{pred}} = \sum_{i=0}^{2L} \mathbf{w}^{a,i} \mathbf{x}_t^{\text{pred},i} \quad (11e)$$

$$\mathbf{x}_t^{\text{pred},i} = \mathbf{x}^{\text{pred}}(\mathbf{y}_t^i) \quad (11f)$$

$$\mathbf{P}_{t|t-1} = \mathbf{C}_y + \sum_{i=0}^{2L} \mathbf{w}^{c,i} (\mathbf{y}_t^i - \hat{\mathbf{y}}_t) (\mathbf{y}_t^i - \hat{\mathbf{y}}_t)^\top \quad (11g)$$

$$\hat{\mathbf{y}}_t = \sum_{i=0}^{2L} \mathbf{w}^{a,i} \mathbf{y}_t^i \quad (11h)$$

$$\mathbf{P}_{t|t} = \mathbf{P}_{t|t-1} - \mathbf{K}_t \mathbf{S}_t \mathbf{K}_t^\top \quad (11i)$$

where \mathbf{y}_t^i with $i = 0, \dots, 2L$ are the sigma points, $\mathbf{w}^{c,i}$ and $\mathbf{w}^{a,i}$ are the weights of the sigma points, \mathbf{C}_t^{sz} is the cross-covariance matrix, \mathbf{S}_t is the innovation covariance, and $\mathbf{P}_{t|t}$ is the estimate covariance. The weights are user defined, and in this paper, we use the same weights as described in *remark 6* of [2]. Lastly, note that the covariance matrix \mathbf{C}_θ (which is initialized by the user) defines the ‘aggressiveness’ of the auto-tuning, while \mathbf{C}_v defines the ‘weight’ given to the components of $\mathbf{x}_t^{\text{ref}}$ [2].

IV. IMPLEMENTATION

A. Computer specifications

Our method was performed on a laptop with 4 CPU cores (Intel core i7-8850H CPU at 2.60 Ghz) with a Quadro P3200 GPU. We note that the computation time of the auto-tuner with the neural network as described in Section III-B was ≈ 0.3 seconds for each update of our control parameters, which includes a time horizon of $N = 20$. However, the computation time of the auto-tuner does increase with either a greater time horizon or number of tuning parameters (i.e., larger neural networks). Although we chose a relatively small network in this work (since we only needed a small network to learn the residual errors for our application), larger networks can still be chosen because the computation time of the auto-tuner is not critical and can be computed (as we do here) on its own CPU core through multi-processing. In other words, the auto-tuner can update parameters at any point during the experiment operation and does not need to be updated at any specific frequency.

B. Differential Drive Robot

We first demonstrate our methods on a differential drive two-wheeled robot as validation (before applying our methods on our manipulator robot). Localization for the real robot is done using April tags on each corner of a 1 by 1 meter square box and on the robot itself, with an Intel RealSense D435i RGB-D camera in a bird’s eye view configuration. The localization provides state estimation of the robot’s position and heading angle in addition to their corresponding velocities. For simulating our robot, we use the Webots software [17] which includes system noise and contact dynamics.

To propagate our states (where the residual error is an error on velocity), we use the following differential drive kinematic equation:

$$\begin{bmatrix} \dot{x}_t \\ \dot{y}_t \\ \dot{\Theta}_t \end{bmatrix} = \begin{bmatrix} \frac{R}{2} V \cos(\Theta_t) & \frac{R}{2} V \cos(\Theta_t) \\ \frac{R}{2} V \sin(\Theta_t) & \frac{R}{2} V \sin(\Theta_t) \\ -\frac{R}{L} & \frac{R}{L} \end{bmatrix} \mathbf{u}_t + \delta f(\mathbf{y}_t) \quad (12)$$

where \dot{x} , \dot{y} , $\dot{\Theta}$ represent the linear and angular velocity (Θ is yaw heading angle), V is a constant angular wheel velocity, R is the radius of the wheel, L is the length from the left to the right wheel, and $\mathbf{u} \in \mathbb{R}^{2 \times 1}$ is the control input for the left (u_t^l) and right (u_t^r) wheel, where the values range from -1 to 1 (depending on whether the robot moves forwards, backwards, or makes a turn clockwise or counterclockwise). Lastly, $\delta f(\mathbf{y}_t)$ represents the residual error predicted by the neural network with auto-tuning (see Section III-B). For the differential drive robot, our input to this neural network is $\mathbf{z}_t = [\dot{x}_t, \dot{y}_t, \dot{\Theta}_t, u_t^l, u_t^r]^\top$. Note, that our residual error is an error on the velocity.

To use the auto-tuning formulation and apply the Kalman gain update as described in equation (9), we will use the following for the differential drive robot:

$$\mathbf{x}_t^{\text{ref}} = \begin{bmatrix} \dot{x}_{t-N|t}^{\text{ref}} C_{\dot{x}} \\ \dot{y}_{t-N|t}^{\text{ref}} C_{\dot{y}} \\ \dot{\Theta}_{t-N|t}^{\text{ref}} C_{\dot{\Theta}} \end{bmatrix}, \hat{\mathbf{x}}_t^{\text{pred}} = \begin{bmatrix} \dot{x}_{t-N|t} C_{\dot{x}} \\ \dot{y}_{t-N|t} C_{\dot{y}} \\ \dot{\Theta}_{t-N|t} C_{\dot{\Theta}} \end{bmatrix} \quad (13)$$

where $\mathbf{x}_t^{\text{ref}}$ is received directly from state estimation of the simulator or the real robot. $\hat{\mathbf{x}}_t^{\text{pred}}$ are the values received from the UKF equations described in (11), and utilizes the kinematic model or the simulator (with the appropriate residual error(s) depending on the test case) from equation (1). Moreover, we also include a cost term, C , on each component of $\mathbf{x}_t^{\text{ref}}$ and $\mathbf{x}_t^{\text{pred}}$ —these costs can (if desired by the user) emphasize learning residual errors of certain components over others (e.g., if the robot’s reference trajectory is composed of mainly turning in place, putting a higher cost $\dot{\Theta}$ may be preferable over other components). In this work, we chose a cost of $C = 1$ for all components and test cases.

C. Manipulator Robot

After validating our methods on the mobile wheeled robot, we then demonstrate our methods on one of the arms of our manipulator robot SCALER [18]. The arm has 6 degrees

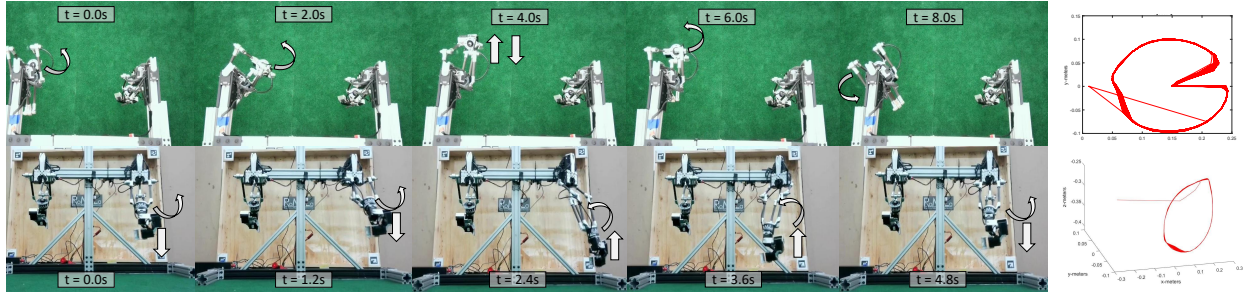


Fig. 4. **Manipulator trajectories.** For evaluating the modelling of residual errors on the manipulator arm, we use two trajectories. The first trajectory (shown in top half) consists of only x and y components—drawing a 2D circle, with a straight line in the middle. This was done to ensure we can model circular and also linear motions simultaneously. The second trajectory, shown on the bottom half, consists of x , y , and z components—drawing a circle in x and y while moving up and down in z . The red line on the last image of the trajectory shows the complete trajectory made by the arm.

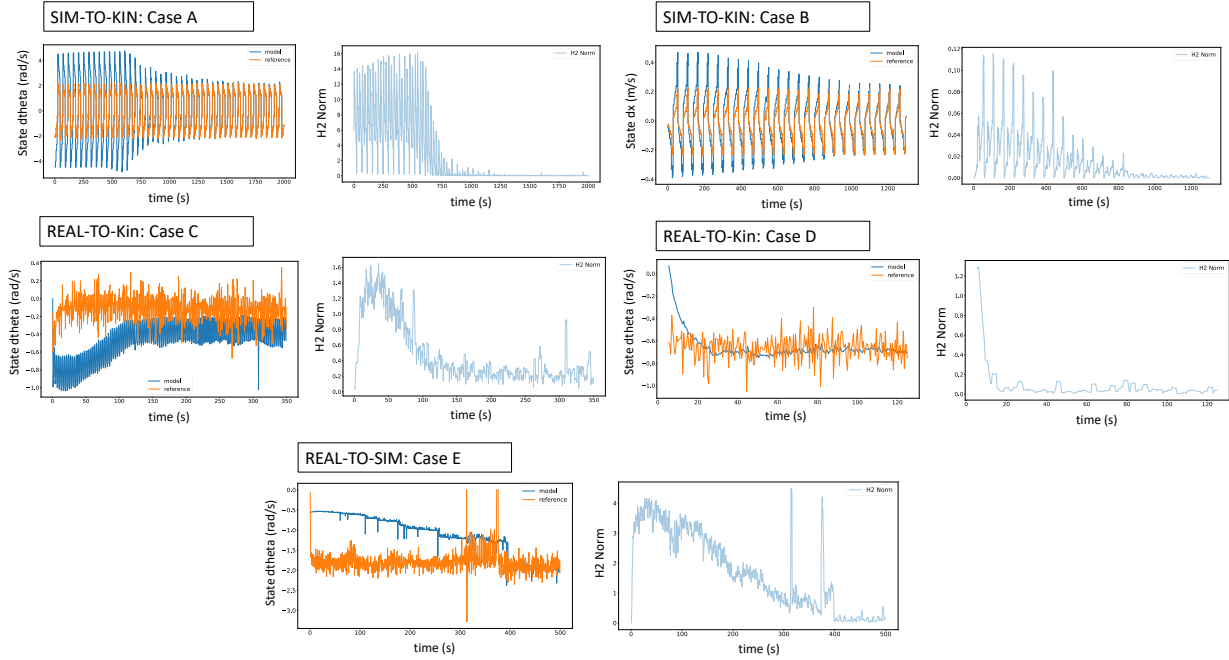


Fig. 5. **Differential drive robot results** The results of learning the residual error of our two-wheeled robot is shown here and described further in Section IV-B. In all cases, the H2 norm converges to a steady-state value near zero, indicating the residual model could be learned. We do note that for the real robot (Case C-E) we observed very noisy data due to our hardware (e.g., the wheels would stick and slip on the ground) and error-prone localization. By using a low-pass filter on the output of our neural network however, we could generate a more robust convergence even for this difficult setup.

of freedom, composed of five-bar linkages combined with a shoulder joint and a spherical wrist joint. Localization for the real robot is done using joint encoders from Dynamixel XM540-w270-T motors placed at each joint. For simulating our robot, we use the PyBullet physics engine [19]. Pybullet is an open source simulator which has been widely used in the robotics field. Taking advantage of the rigid body dynamics constraint solver in Pybullet, we simulate the manipulator robot with a closed loop kinematics chain. In the simulator, we use the in-built position control to control the actuators, and set the simulation time step to be 0.01 seconds. Our objective will be to add the residual error in task space (i.e., on end-effector velocities). The velocities in task space are then used as part of our estimation of $\hat{\mathbf{x}}_t^{\text{pred}}$, and as was done in the implementation of the differential

drive robot, compared to the reference value $\mathbf{x}_t^{\text{ref}}$. Thus, to propagate the states of our manipulator robot, we have:

$$\begin{bmatrix} \dot{x}_t \\ \dot{y}_t \\ \dot{z}_t \end{bmatrix} = \frac{FK(\boldsymbol{\theta}_{t-1} + \dot{\boldsymbol{\theta}}_{t-1}\Delta T) - FK(\boldsymbol{\theta}_{t-1})}{\Delta T} + \delta f(\mathbf{y}_{t-1}) \quad (14)$$

where $FK(\boldsymbol{\theta}_{t-1})$ represents the forward kinematics of our manipulator robot with joint angles $\boldsymbol{\theta}_t \in \mathbb{R}^{6 \times 1}$, joint velocities $\dot{\boldsymbol{\theta}}_t \in \mathbb{R}^{6 \times 1}$, and \dot{x}_t , \dot{y}_t , and \dot{z}_t are the end-effector velocities (a Jacobian can also be used in place of our differentiation). The residual error, $\delta f(\mathbf{y}_t)$, to be predicted by the neural network with auto-tuning (see Section III-A) for the manipulator robot, will have the input $\mathbf{z}_t = [\dot{\theta}_{t,1}, \dot{\theta}_{t,2}, \dot{\theta}_{t,3}, \dot{\theta}_{t,4}, \dot{\theta}_{t,5}, \dot{\theta}_{t,6}]^\top$, where $\dot{\theta}_{t,1} - \dot{\theta}_{t,3}$ are the shoulder joint velocities, and $\dot{\theta}_{t,4} - \dot{\theta}_{t,6}$ are the spherical

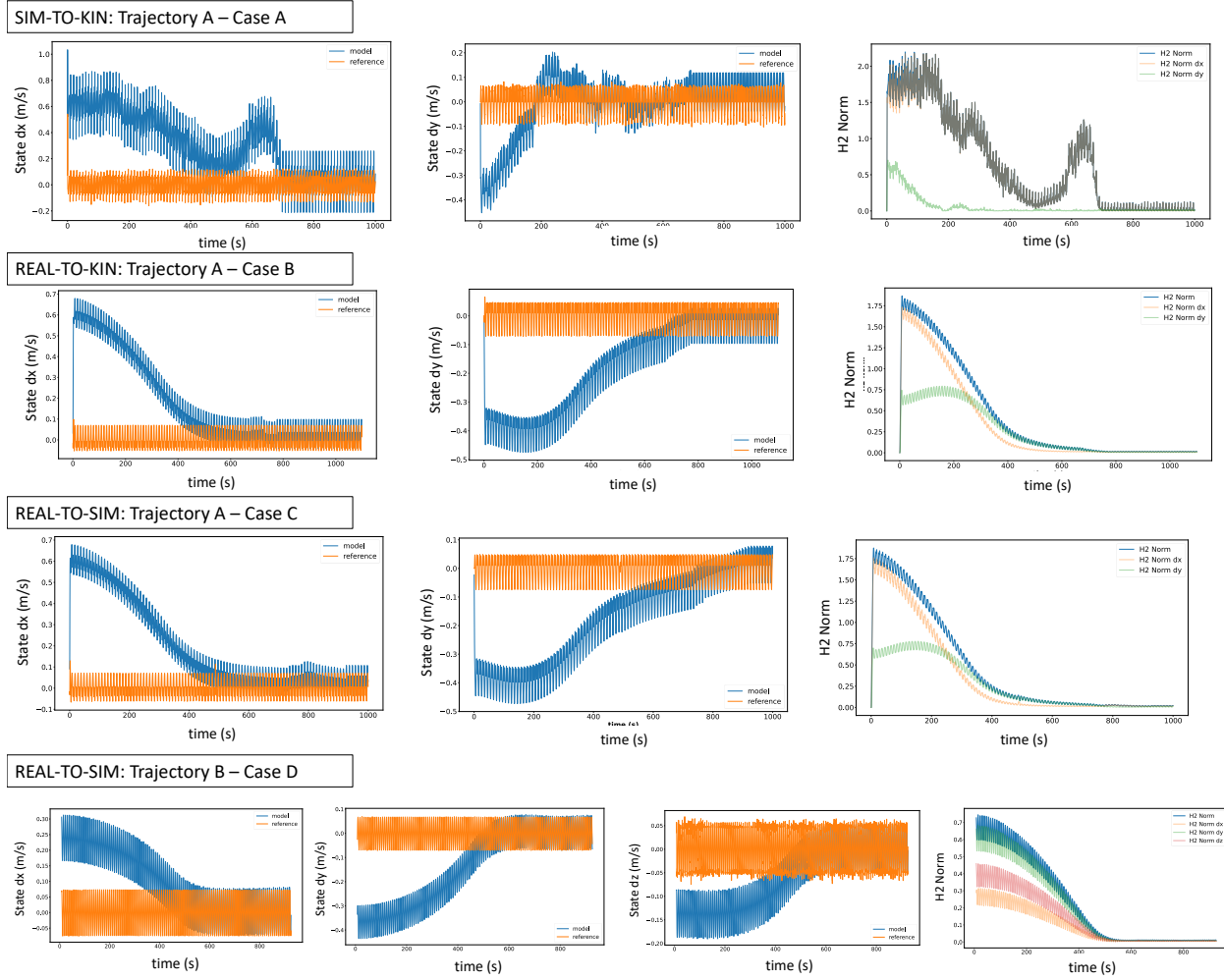


Fig. 6. **Manipulator arm results.** The results of learning the residual error of our manipulator robot is shown here, and described in more detail in Section IV-B. For the manipulator arm, we use two trajectories (one consists of 2D motion, i.e., Cases A-C, while another demonstrates 3D motion, i.e., Case D). The motion is described and visualized in Fig. 4. Overall, the H2 norm decreased for all cases. We also not only show the overall H2 norm but also the H2 norm of each individual component (i.e., \dot{x} , \dot{y} , and \dot{z}). Unlike the case for our wheeled robot, the localization of our manipulator arm was more stable (we used encoders for localization) and did not require any additional filters to our outputs.

joint velocities. Similar to equation (13) for the differential drive robot, we have the following definitions for $\hat{\mathbf{x}}_t^{\text{pred}}$ and $\hat{\mathbf{x}}_t^{\text{ref}}$ (with cost $C = 1$ for our case):

$$\mathbf{x}_t^{\text{ref}} = \begin{bmatrix} \dot{x}_{t-N|t}^{\text{ref}} C_{\dot{x}} \\ \dot{y}_{t-N|t}^{\text{ref}} C_{\dot{y}} \\ \dot{z}_{t-N|t}^{\text{ref}} C_{\dot{z}} \end{bmatrix}, \hat{\mathbf{x}}_t^{\text{pred}} = \begin{bmatrix} \dot{x}_{t-N|t} C_{\dot{x}} \\ \dot{y}_{t-N|t} C_{\dot{y}} \\ \dot{z}_{t-N|t} C_{\dot{z}} \end{bmatrix} \quad (15)$$

V. EXPERIMENTAL RESULTS

Our results are demonstrated for the mobile wheeled robot in Fig. 5 and for our manipulator robot in Fig. 6. For both robots, we evaluate the results of our method by comparing the current model (i.e., kinematic or simulator model) with a reference model (simulator model or the real robot) by calculating the H2 Norm for each time step during the training process (i.e., defined as $\|\mathbf{x}_t^{\text{ref}} - \mathbf{x}_t^{\text{pred}}\|$). Thus, if the H2 norm decreases over time and reaches a steady-state value (ideally close to zero), we can assume convergence of the auto-tuning procedure. In Fig. 5, we show that the

H2 norm decreases for each test case (in light blue) which is estimated based on the model values (dark blue) and reference values (orange). A and B present the Sim-to-Kin cases, where in A we use a reference trajectory where the robot spins in place and $\dot{\theta}$ changes from -2 to 2 rad/s, and in B we use a reference trajectory that drives the robot back and forth in the x -direction (where \dot{x} ranges from -0.2 to 0.2 m/s). The Real-to-Kin cases are shown in C and D (both used a reference trajectory which only changes the angular velocity). However, we note that for the real robot we faced several issues due to localization and hardware. For example, the localization would at times cause large amplitude spikes when estimating the state, and our wheeled robot was made out of cheap material causing sticking and slipping behavior (as seen by the orange graph in case C). This noise affected the predicted model produced by our auto-tuner (graph in blue), which still managed to converge but to a local optima solution (as shown by the offset). One option is to introduce a low-pass filter, which we applied

on the predicted model output as seen in Case D (we could have also applied the filter on the localization output instead, however, this would not demonstrate as strong of a case for controller robustness under large uncertainty). With the filter, we show a convergence without offset. Lastly, we test the Real-to-Sim case in E (using the filter as done in D) and with a reference trajectory that imposes a constant angular velocity. Some spikes are observed (likely due to bad localization values as seen in the graph in orange) but was able to converge within approximately 17 minutes. We note that we could not test the x or y direction for the real robot cases due to our limited hardware environment (the robot does not stay in place even when turning, and the localization with our camera setup provided a very minimal workspace, not allowing for longer linear motion—thus, we could only test linear motion for the wheeled robot for the simulation cases as shown in A and B. However, we do test linear and circular motion in a 3D environment using our manipulator arm instead (which is not constricted by the environment).

The results from using our manipulator robot are shown in Fig. 6. For cases A - C we used the same reference trajectory as illustrated in top half of Fig. 4 (circular 2D motion and drawing a line through the circle—this trajectory was chosen as transferring from circular to linear motion causes additional residual error, which we plan to account for with our methods). Note, that the Real-to-Kin case (or B) produced more robust results (i.e., less transient errors) compared to the Sim-to-Kin case (or A). One explanation is that as formulated in equation (4), the residual model error trained in the Sim-to-Kin case is used as part of the formulation in equation (4). Thus, this additional knowledge may serve as a good initialization for the auto-tuner when training the next test case. Finally, we demonstrate two Real-to-Sim cases (C and D), where C is trained on the same reference trajectory as A-B, and D is trained on a reference trajectory shown in bottom half of Fig. 4 (A circle for the x , and y components and moving up and down in z). In both of these cases, the H2 norm reaches near zero and converges. Lastly, we note that convergence typically occurs at approximately 8 minutes.

VI. CONCLUSION

In this paper we demonstrated a method that can learn and predict the residual model errors between Kinematic/Simulator models and the real robot. Approximately 17 minutes of experimental data for the wheeled robot and 8 minutes of experimental data for the manipulator robot was required to achieve convergence (i.e., learn the residual model error). Thus, this method is feasible for employment on hardware and with sparse amounts of data. Although the wheeled robot imposed severe hardware limitations (i.e., wheels would stick/slide on the surface), and we required low-pass filtering to generate more robust convergence (although convergence was received even without filters), this result showed that experimenting with filtering techniques as part of the tuning process may be promising to increase robustness. Other future work includes applying our method

for more complex tasks (i.e., modelling residual error while grasping an object) and legged systems (i.e., quadrupeds and bipeds), and employing larger neural network structures that consists of more challenging data-types (i.e., vision-based data).

REFERENCES

- [1] W. Zhao, J. P. Queralta, and T. Westerlund, "Sim-to-real transfer in deep reinforcement learning for robotics: a survey," in *2020 IEEE Symposium Series on Computational Intelligence (SSCI)*, 2020, pp. 737–744.
- [2] M. Menner, K. Berntorp, and S. D. Cairano, "A Kalman filter for online calibration of optimal controllers," in *2021 IEEE Conf. on Control Tech. and Applic. (CCTA)*, 2021, pp. 441–446.
- [3] Y. Du, O. Watkins, T. Darrell, P. Abbeel, and D. Pathak, "Auto-tuned sim-to-real transfer," in *2021 IEEE International Conference on Robotics and Automation (ICRA)*, 2021, pp. 1290–1296.
- [4] B. Mehta, M. Diaz, F. Golemo, C. J. Pal, and L. Paull, "Active domain randomization," in *CoRL*, 2019.
- [5] OpenAI, I. Akkaya *et al.*, "Solving rubik's cube with a robot hand," 2019. [Online]. Available: <https://arxiv.org/abs/1910.07113>
- [6] Y. Chebotar *et al.*, "Closing the sim-to-real loop: Adapting simulation randomization with real world experience," in *2019 International Conference on Robotics and Automation (ICRA)*, 2019, pp. 8973–8979.
- [7] M. Deisenroth and C. Rasmussen, "Pilco: A model-based and data-efficient approach to policy search," in *Proceedings of the 28th International Conference on Machine Learning (ICML-11)*, ser. ICML '11, L. Getoor and T. Scheffer, Eds. New York, NY, USA: ACM, June 2011, pp. 465–472.
- [8] H. Durrant-Whyte, N. Roy, and P. Abbeel, *Learning to Control a Low-Cost Manipulator Using Data-Efficient Reinforcement Learning*, 2012, pp. 57–64.
- [9] R. Jeong *et al.*, "Self-supervised sim-to-real adaptation for visual robotic manipulation," 2019. [Online]. Available: <https://arxiv.org/abs/1910.09470>
- [10] P. Pastor *et al.*, "Learning task error models for manipulation," in *2013 IEEE International Conference on Robotics and Automation*, 2013, pp. 2612–2618.
- [11] U. Hubert, J. Stückler, and S. Behnke, "Bayesian calibration of the hand-eye kinematics of an anthropomorphic robot," in *2012 12th IEEE-RAS International Conference on Humanoid Robots (Humanoids 2012)*, 2012, pp. 618–624.
- [12] S. Aoyagi *et al.*, "Improvement of robot accuracy by calibrating kinematic model using a laser tracking system-compensation of non-geometric errors using neural networks and selection of optimal measuring points using genetic algorithm-," in *2010 IEEE/RSJ International Conference on Intelligent Robots and Systems, October 18-22, 2010, Taipei, Taiwan*. IEEE, 2010, pp. 5660–5665. [Online]. Available: <https://doi.org/10.1109/IROS.2010.5652953>
- [13] R. Vrabčič *et al.*, "An architecture for sim-to-real and real-to-sim experimentation in robotic systems," *Procedia CIRP*, vol. 104, pp. 336–341, 2021, 54th CIRP CMS 2021 - Towards Digitalized Manufacturing 4.0. [Online]. Available: <https://www.sciencedirect.com/science/article/pii/S2212827121009550>
- [14] A. Dalla Libera, N. Castaman, S. Ghidoni, and R. Carli, "Autonomous learning of the robot kinematic model," *IEEE Transactions on Robotics*, vol. 37, no. 3, pp. 877–892, 2021.
- [15] A. Schperberg, S. D. Cairano, and M. Menner, "Auto-tuning of controller and online trajectory planner for legged robots," *IEEE Robotics and Automation Letters*, pp. 1–8, 2022.
- [16] A. Schperberg, Y. Shirai, X. Lin, Y. Tanaka, and D. Hong, "Auto-calibrating admittance controller for robot motion of robotic systems," *arXiv preprint arXiv:2207.01033*, 2022.
- [17] O. Michel, "Webots: Professional mobile robot simulation," *Journal of Advanced Robotics Systems*, vol. 1, no. 1, pp. 39–42, 2004. [Online]. Available: <http://www.ars-journal.com/International-Journal-of-Advanced-Robotic-Systems/Volume-1/39-42.pdf>
- [18] Y. Tanaka *et al.*, "Scaler: A tough versatile quadruped free-climber robot," *Proc. 2022 IEEE/RSJ Int. Conf. Intell. Rob. Syst.*, 2022.
- [19] B. Ellenberger, "Pybullet gymperium," <https://github.com/benelot/pybullet-gym>, 2018–2019.